

# We are IntechOpen, the world's leading publisher of Open Access books Built by scientists, for scientists

6,900

Open access books available

186,000

International authors and editors

200M

Downloads

Our authors are among the

154

Countries delivered to

TOP 1%

most cited scientists

12.2%

Contributors from top 500 universities



WEB OF SCIENCE™

Selection of our books indexed in the Book Citation Index  
in Web of Science™ Core Collection (BKCI)

Interested in publishing with us?  
Contact [book.department@intechopen.com](mailto:book.department@intechopen.com)

Numbers displayed above are based on latest data collected.  
For more information visit [www.intechopen.com](http://www.intechopen.com)



## Chapter

# Fuzzy Photogrammetric Algorithm for City Built Environment Capturing into Urban Augmented Reality Model

*Igor Agbossou*

## Abstract

Cities are increasingly looking to become smarter and more resilient. Also, the use of computer vision takes a considerable place in the panoply of techniques and algorithms necessary for the 3D reconstruction of urban built environments. The models thus obtained make it possible to feed the logic of decision support and urban services thanks to the integration of augmented reality. This chapter describes and uses Fuzzy Cognitive Maps (FCM) as computing framework of visual features matching in augmented urban built environment modeling process. It is a combination of the achievements of the theory of fuzzy subsets and photogrammetry according to an algorithmic approach associated with the ARKit renderer. In this experimental research work, part of which is published in this chapter, the study area was confined to a portion of a housing estate and the data acquisition tools are in the domain of the public. The aim is the deployment of the algorithmic process to capture urban environments built in an augmented reality model and compute visual feature in stereovision within FCM framework. The comparison of the results obtained with our approach to two other well-known ones in the field, denotes the increased precision gain with a scalability factor.

**Keywords:** fuzzy cognitive maps, fuzzy sets, photogrammetry, urban augmented reality model, fuzzy stereovision matching constraints

## 1. Introduction

The use of advanced scientific computation methods and techniques is classic in geography, land use and regional planning [1–8]. Indeed, the study and analysis of geographical spaces such as cities for example, which themselves have acquired the qualification of complex system [1, 2, 5, 9–14] are an illustration of this classic usage [15–24]. Among these scientific computational approaches is also fuzzy inference logic [21, 22, 25, 26]. As part of the research work reported in this chapter, we relied on the scientific achievements of fuzzy inference systems [27–30] to integrate into our methodological approach Fuzzy Cognitive Maps (FCM) [31–34] in the process of

visual features matching computation. It's applied through the collection of captured photography of urban built environment to build an augmented urban reality model [35–40].

Thereby, thematic analyzes of built urban environments require the acquisition of 3D urban landscape data, street furniture and several other real visual data. The data to be processed are bi-dimensional (2D) images captured from the tri-dimensional (3D) scene. The objects in 3D are generally composed of related parts that joined from the whole object. In computer graphics, we usually use a specialized software, for instance, Maya [41] or Blender [42, 43] to interactively create models or procedural 3D modeling [44–48] which creates a mathematical representation of a 3D object. It is common to use a few photographs as references and textures to generate models using a modeling tool. When it comes to 3D modeling and urban spaces [49–51], the more systematic introduction of photographs as input to generate a photorealistic 3D model of a built environment is called « Image-based Modeling » [52] and can generate models for objects physically existing. More importantly, such a modeling process can be automated, and therefore can be scaled up for applications [52]. More fundamentally, how to recover the lost third dimension of objects from a collection of 2D images is one of the main objectives of computer vision [53] and the technical challenge resolved in this work. Fortunately, the relations in 3D are preserved in 2D [42, 44, 45, 47, 54]. Hence, we can exploit this fact by considering specific and basic elements which are related to other elements in the 2D images. Those specific and basic elements are stereo correspondence features: epipolar [55], similarity [56], smoothness [57], ordering [58] and uniqueness [59].

Indeed, the use of photogrammetry, which is a technique that consists of taking measurements in a scene, using the parallax obtained between images acquired from different points of view, proves to be an excellent approach for producing captures that conform to the reality [53]. To better manage the parallax during the 3D reconstruction, we combined fuzzy classification algorithm [8, 60, 61] to the photogrammetric processing within the framework of the well-established soft computing technique called Fuzzy Cognitive Map (FCM) [62–67]. Our Fuzzy Photogrammetric Algorithm Kernel (FPAK) applied to 3D reconstruction from images precisely becomes the meeting point of computer graphics and vision, with the finalized 3D representation of urban built environment.

The rest of the chapter is organized as follows: Section 2 presents background of FCM and its mathematical formalization we adopted [22]. Section 3 expose the core of this chapter: materials and methods. Section 4 presents with the experimental results obtained. The conclusion of the chapter puts lights on the future.

## **2. FCM background**

Well-developed modeling methodology for complex systems that allow to describe the behavior of a system in terms of concepts, Fuzzy Cognitive Maps (FCM) are powerful tools for modeling dynamic systems that was introduced by Kosko [32, 68, 69]. The resulting model describes expert knowledge (semantic concepts and/or computed values for example) of complex systems with high dimensions and a variety of factors. The scientific community is expressing a growing interest about the theory and application of FCMs in complex systems, and their validity and usefulness has been proved in various fields [22, 62–67, 70, 71]. FCMs are fuzzy causality

backpropagation approach of modeling which combine fuzzy logic, nonlinear computing, semantic and neural networks.

2.1 Theoretical foundation of FCM

FCMs are fuzzy signed directed graphs with feedback. They are appropriate to encode knowledge thanks to concepts organized and causally linked to each other with weightings. Each concept is materialized by a network node. Different FCM networks have been used as a decision modeling tool under different approaches [63–67, 72]. FCMs are based on the theory of fuzzy logic and fuzzy subsets, thus improving the ability of cognitive maps to present and model qualitatively and quantitatively dynamic nonlinear systems. So, FCM is a soft computing modeling technique used for dynamic causal knowledge acquisition and process reasoning. Under its most general approach, each concept represents an entity, a state, a variable, or a feature of the system. An FCM embeds the topology of a fuzzy signed direct graph and a nonlinear neural networks feedback dynamic [26, 33, 61]. Concepts are equivalent to neurons which state value is not binary but belongs to a fuzzy subset. The value  $w_{ij}$  of the directed edge from causal concept  $C_i$  to concept  $C_j$  measures how much  $C_i$  causes  $C_j$ . Value  $w_{ij}$  belongs the fuzzy causal interval  $[-1, +1]$ ,  $w_{ij} = 0$  indicates no causality;  $w_{ij} > 0$  indicates causal increase, this means that  $C_j$  increases as  $C_i$  increases and vice versa,  $C_j$  decreases as  $C_i$  decreases;  $w_{ij} < 0$  indicates causal decrease or negative causality.  $C_j$  decreases as  $C_i$  increases and  $C_j$  increases as  $C_i$  decreases.

Depending on the direction and size of this effect, and on the threshold levels of the dependent concepts, the affected concepts may subsequently change their state as well, thus activating further concepts within the network. Because FCMs allow feedback loops, newly activated concepts can influence concepts that have already been activated before. As a result, the activation spreads in a nonlinear fashion through the FCM net until the system reaches a stable limit cycle or fixed point.

2.2 FCM representation

To illustrate the description made above of FCMs, we will consider one, composed of 5 concepts and 10 causality links in total as shown in **Figure 1**. Concepts variables are represented by nodes, such as  $C_1$ ,  $C_2$ ,  $C_3$ ,  $C_4$  and  $C_5$ .

In the relation  $C_1 \rightarrow C_2$ ,  $C_1$  is said to impact  $C_2$ . So,  $C_1$  is the causal variable, whereas  $C_2$  is the effect variable, and the intensity of the causality is expressed by the value of  $w_{12}$ . Also, in the relation  $C_2 \rightarrow C_1$ ,  $C_2$  is said to impact  $C_1$ , and the intensity of the causality is expressed by the value of  $w_{21}$ . Each concept is characterized by a

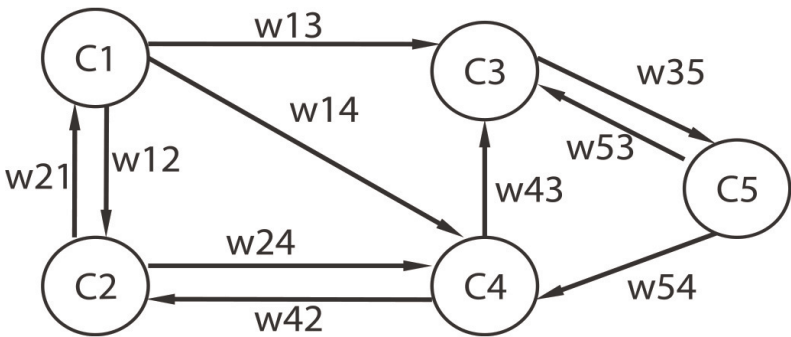


Figure 1.  
Simple fuzzy cognitive map model illustration.

number  $A_i$  that results from its computed value through the transformation of the real value of the hole system's variables.

There are 3 possible types of causal relationships between concepts:

- $w_{ij} > 0$  which indicates positive causality between two concepts.
- $w_{ij} < 0$  which indicates negative causality between two concepts.
- $w_{ij} = 0$  which indicates the absence of causality between two concepts.

The value of  $w_{ij}$  indicates how strongly concept  $C_i$  influence concept  $C_j$ . The sign of  $w_{ij}$  indicates whether the relationships between concept  $C_i$  and  $C_j$  is direct or inverse. The direction of causality indicates whether concept  $C_i$  causes concept  $C_j$  or vice versa. These parameters must be considered when a value is assigned to weight  $w_{ij}$ .

### 2.3 Mathematical formalization of FCM

The operation of FCMs is based on an inferential process whose dynamics can be formalized mathematically. A FCM model acts as a network of threshold or continuous concepts [64, 66, 68, 69]. At this level, they differ from a simple neural network because they are based on extracting knowledge from experts [33, 64, 73] and do not require a data input layer. The nonlinear structure of each concept is expressed during the dynamics of the whole system through backpropagation [74, 75]. Then, the value  $A_i^{t+1}$  for each concept  $C_i$  at each time step is calculated [22, 65, 74] by the following general rule:

$$A_i^{t+1} = f \left( k_1 \sum_{\substack{j=1 \\ j \neq i}}^n W_{ji} A_j^t + k_2 A_i^t \right) \quad (1)$$

The  $k_1$  expresses the influence of the interconnected concepts in the configuration of the new value of the concept  $A_i$  and  $k_2$  represents the proportion of the contribution of the previous value of concept in the computation of the new value. This formulation assumes that a concept links to itself with a weight  $w_{ii} = k_2$ . Namely,  $A_i^t$  and  $A_i^{t+1}$  are respectively the values of concept  $C_i$  at times  $t$  respectively  $t + 1$ .  $w_{ji}$  is the weight of the interconnection from concept  $C_j$  to concept  $C_i$  and  $f$  is a threshold function defined in Eq. (2). The unipolar sigmoid function is the most used threshold function [57, 65, 67] where  $\lambda > 0$  determines the steepness of the continuous function  $f$ . For the purposes of this research, the value of  $\lambda$  is fixed at unity, i.e. 1. The sigmoid function ensures that the calculated value of each concept will belong to the interval  $[0,1]$ .

$$f(x) = \frac{1}{1 + e^{-\lambda x}} \quad (2)$$

## 3. Materials and methods

Physical based rendering 3D simulation of large-scale urban built environment processes is one of greatest challenges of modern computing techniques in urban



studies and regional planning [17, 39, 47, 50]. In fact, urban systems are naturally complex by own [1–5, 14]. Simulation allows us to understand the reasons and effects of events and situations in a real system. Moreover, it allows us to predict the results of actions on future states of the system. The level of detail [15, 39, 45, 50] between simulation results and real system behavior depends on the model used. More-precise models with large data may reflect reality in a more-precise manner; however, the complexity directly influences the time required to compute model changes.

### 3.1 Urban study area

The model created in this study covers a portion of a new housing estate under construction in the town of Belfort in France. The area of the development project for building individual houses has 25 plots of 600 to 900 m<sup>2</sup>. **Figure 2** provides an overview of the area called “Jardins du MONT”.

Indeed, it is a real estate program whose architecture of the houses is contemporary, of high quality and of superior range located less than 10 minutes by car, bus, or bike from the city center of Belfort. We are also less than 10 minutes’ walk from the heart of the “Techn’Hom” business park (GE, Alstom...), one of the economic lungs of the town, with an exceptional view of Belfort, its fortifications and the surroundings, all integrated in a green, calm and privileged urban setting.

The general framework of our research work includes 3D spatial analysis, the temporal evolution of new housing estates and the deployment of smart cities, with scientific tools in artificial intelligence. Also, it seemed legitimate to us to take an interest in this portion of the city under construction to experiment with our approach which is the subject of this chapter: create an augmented reality scene model of the built environment through the combination of photogrammetry [76–81] and fuzzy modeling techniques.

### 3.2 Sensor for data acquisition

In addition to the question of costs, the spatial scale of the data to be collected as well as the expected quality dictate the choice of tools to be preferred. There are

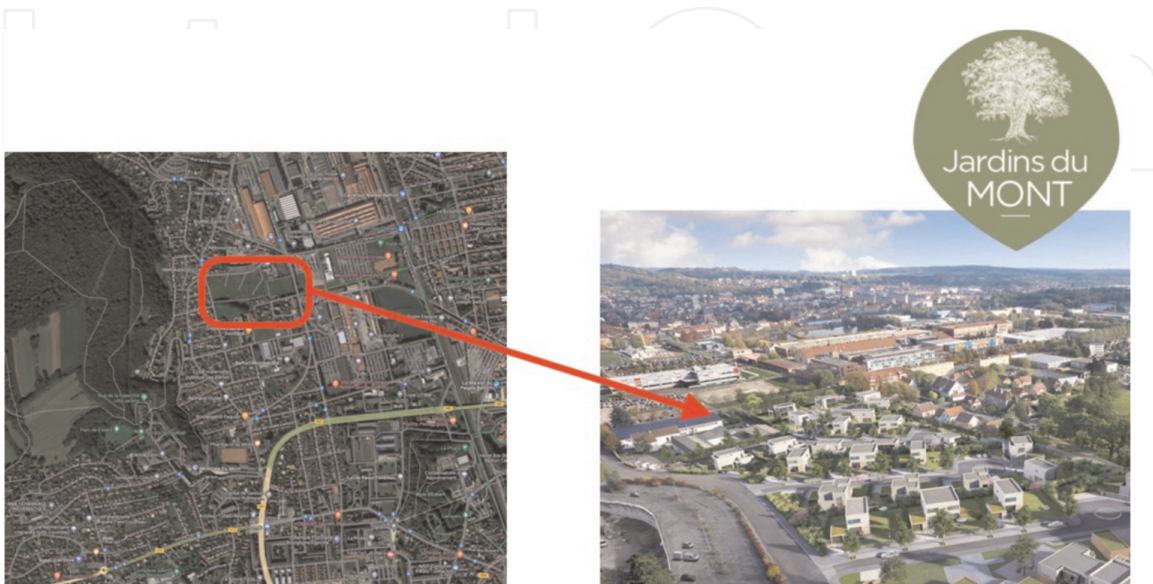


**Figure 2.**  
Urban study area “Jardins du MONT”, Belfort (France).

several tools for Geodata collection [38, 49]: Total Stations, Global Navigation Satellite System (GNSS) receivers, Light Detection and Ranging (LiDAR) scanner, Static Terrestrial Laser Scanning (STLS), Airborne Laser Scanning (ALS), Helicopter Laser Scanning (HLS), Mobile Laser Scanning (MLS), Drone, Tablets and Smartphones. As part of this experimental study, we use portable and mobile sensor which smartphones are equipped with. And for good reason, the sensors of these modern devices perfectly meet the requirements relating to the acquisition of data for photogrammetry [82]. Range (or depth) data is crucial for understanding and working with the 3D scene projected onto a 2D plane forming an image. There are multiple ways to obtain such information [83–87], either using a depth sensor or estimating depth. A depth sensor is a device that provides the distance from the sensor to an element in the scene, although it is possible to collect distance information using two or more RGB cameras from a scene.

Due to its following features: wide color capture for photos and live photos, lens correction, retina flash, auto image stabilization, burst mode, etc. we used the iPhone 13 Pro Max as a sensor for acquiring images to feed the model. **Figure 3** illustrates it.

### 3.3 Data collection principles and quality requirements

When capturing images for augmented reality, we use a large part of the image sensor. To be more precise, it's an area of  $3840 \times 2880$  pixels on the iPhone 13 Pro. Then, we use a process called binning [88, 89]. It works as follows: Binning takes a region of  $2 \times 2$  pixels, averages the pixel values, and writes back a single pixel. This has two significant advantages. First, image dimensions are reduced by a factor of two, in this case, it downscales to  $1920 \times 1440$  pixels. As a result of this, each frame consumes way less memory and processing power. This allows the device to run the camera at up to 60 frames per second and frees up resources for rendering. Secondly, this process offers an advantage in low light environments, where the averaging of pixel values reduces the effects of sensor noise.

Images captured by a camera are geometrically warped by small imperfections in the lens. To project from the 2D image plane back into the 3D world, the images must be distortion corrected, or made rectilinear. Lens distortion is modeled using a one-dimensional lookup table of 32-bit float values evenly distributed along a radius from the center of the distortion to a corner, with each value representing a magnification of the radius. This model assumes symmetrical lens distortion [88].

Capturing scenes with iPhone is a computer vision technology that one can leverage to easily turn images of real-world objects into detailed 3D models. We begin by



**Figure 3.**  
*iPhone 13 pro max used as sensor for data acquisition.*

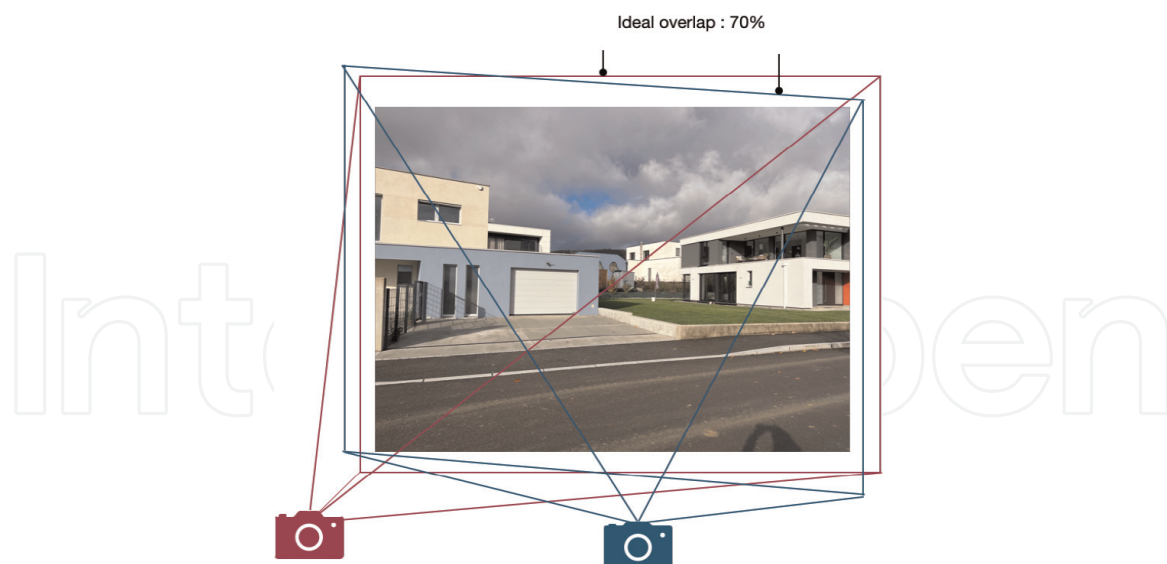


**Figure 4.**  
 Ideal overlap to respect when capturing built environment.

taking photos of the urban built environment from various angles with an iPhone. To photograph all the area with the ability to match landmarks between images we must move the camera around, taking photographs from different angles at different heights.

To ensure landmarks matching between overlapping photographs, camera settings must be consistent as possible from shot to shot. **Figure 5** illustrates a sample of captured data. The reading direction of the photos is indicated there: start-end.

The number of pictures need to create an accurate 3D representation varies depending on the quality of the pairs of photographs making up the sequences in the collection, the complexity and size of the built environment. In addition, adjacent shots must have substantial overlap. So, we position sequential images, so they have a 70% overlap or more ( $0.7 \leq \text{overlap} \leq 0.9$ ) as illustrated in **Figure 4**. Anything less than 50% overlap between neighboring shots, and the 3D reconstruction process may fail or result in a low-quality augmented reality model [15, 52]. Doing an aperture setting narrow enough to maintain a crisp focus is recommended [53, 58]. The spatial precision between the pairs of images and the chromatic density of the textures are a guarantee of the quality of the images collected for the 3D reconstruction of built urban environments. Accordingly, key factors ensuring good quality of input data [15, 52, 53, 58, 90] are summarized in **Table 1**.

Our photographic database is made up of 800 photos taken in compliance with the overlap constraints to feed the model. The entire collection is organized into 799 image pairs. A first step consists in sorting the truly calibrated image pairs according to the constrained constraints of the stereovision image matching.

### 3.4 Image matching in stereovision within FCM framework

The image matching in stereovision [89, 91–94] is the process of identifying the corresponding points in two images that are cast by the same physical point in the tri-dimensional space. This can be carried out pixel by pixel or identifying significant features in the images, such as edges, regions or interest points.

Hence, the stereo correspondence problem can be defined in terms of finding pairs of true matches, namely, pairs of edge segments in two images that are generated by





**Figure 5.**  
*Sample of captured urban built environment dataset*

Factor	Description	Fuzzy threshold value
Range or depth	Distance between camera and scene	Low
Sensor quality	The resolution of de sensor	High
Overlap	Superposition rate between two consecutive photographs	$0.7 \leq \text{overlap} \leq 0.9$
Image texture	Texture and texture variance	High

**Table 1.**  
*Key factors affecting photogrammetric input images quality.*

the same physical edge segment in space. These true matches generally satisfy some constraints:

- 1.epipolar, given two segments one in the left image and a second in the right one, if we slide one of them along a horizontal direction, i.e. parallel to the epipolar line, they would intersect (overlap) (**Figure 4**);

2. similarity, matched edge segments have similar properties or attributes;
3. smoothness, disparity values in a given neighborhood change smoothly, except at a few depth discontinuities;
4. ordering, the relative position among two edge-segments in the left image is preserved in the right one for the corresponding matches;
5. uniqueness, each edge-segment in one image should be matched to a unique edge-segment in the other image.

A large parallax factor value causes the background to move more slowly compared to the foreground. A small value makes the foreground and background move at a similar pace. The parallax effect becomes more apparent as the value of parallax factor increases.

According to FCM framework, causal concepts and their activation levels, the system receives as inputs a pair of stereo images left,  $I_l$  and right  $I_r$ . This pair is processed to extract edge segments and their attributes; each pair of extracted features vectors  $(\vec{e}_{I_l}, \vec{e}_{I_r})$  is to be matched, the vectors  $\vec{e}_{I_l}$  and  $\vec{e}_{I_r}$  come from  $I_l$  and  $I_r$  respectively. For each pair  $(\vec{e}_{I_l}, \vec{e}_{I_r})$  the attribute difference vector  $\vec{x}$  is computed. In this approach, a pair of edge attributes  $(\vec{e}_{I_l}, \vec{e}_{I_r})$  defines a causal fuzzy concept  $C_i$ . The Eq. (1) is applied and the initial activation level at the iteration  $t = 0$  is derived from  $\vec{x}$  as follows in Eq. (3):

$$A_i^0 = \frac{1}{1 + \|\vec{x}\|} \quad (3)$$

where  $\|\vec{x}\|$  is defined as the Euclidean norm. This implies the application of the similarity Gestalt's principle. Hence, our FCM structure is built with as many concepts as pairs of edge attributes, from  $L_l$  and  $L_r$ , are available. The algorithm is synthesized as follows in **Table 2**.

The correspondence results within the pairs for each of the characteristics are recorded in **Table 3** in number of pairs according to the number of iterations:

It is noted that from iteration n°20 the results remain stable. To test the consolidation of these, we have pushed the number of iterations to 35 without any disruption of stability.

In view of these results of this correspondence calculation phase, only the 744 pairs of photographs respecting the five constraints (epipolar, similarity, smoothness ordering and uniqueness) have been selected to now feed the scene of the augmented urban reality model.

## 4. Experimental results

We present in this section, the first significant results of the construction of an Urban Augmented Reality (UAR) scene model resulting from the combination of photogrammetry and fuzzy modeling techniques for future analyses. In our

1. Initialization	Load each concept with its activation level $A_i^{t=0}$ through the Eq. (3); Set: $\delta = 0.05$ , the minimum value of change in classification approach $t_{\max} = 50$ , maximum of iterations $\alpha = 0.9$ , which is the limit indicator of concepts looping in the q network. $nc$ : integer, the number of concepts from a total of q representing pairs of edge attributes that change their activation level at each iteration. The activation mechanism is that defined in Eq. (1)
2. FCM process	$t = 0$ while ( $t < t_{\max}$ and $nc/q < \alpha$ ) { $t \leftarrow t + 1; nc \leftarrow 0$ for (each concept $C_i$ ) { update $A_i^t$ according to Eq. (1) if ( $ A_i^{t+1} - A_i^t  > \alpha$ ) { $nc \leftarrow nc + 1$ } } }
3. Output	The activation levels $A_i^t$ for all concepts updated.

**Table 2.**  
*Process of image matching in stereovision within FCM framework.*

Number of iterations	Epipolar	Similarity	Smoothness	Ordering	Uniqueness
10	788	791	685	778	746
15	790	792	734	783	767
20	791	796	744	785	779
25	791	796	744	785	779
30+	791	796	744	785	779

**Table 3.**  
*Image matching in stereovision within FCM framework results.*

incremental validation process, we rely on two major works [64, 87, 93, 95] to assess the performance of our method and its robustness for large-scale deployment.

4.1 The urban augmented reality model scene

Based on the 744 image pairs, the total number of photographs therefore amounts to 745. The prodigiously increased computing capacities of mobile devices open opportunities for augmented reality applications. The FPAK we developed enables the conversion of urban built environment photos into Urban Augmented Reality (UAR) model as illustrated with **Figure 6**. To achieve AUR, we use the kernel in conjunction with Apple ARKit [96] and RealityKit [97] frameworks. The use of RealityKit framework let implement high-performance 3D simulation and rendering. It leverages information provided by the ARKit framework to seamlessly integrate virtual urban built environment into the real world. In turn, the kernel mainly focuses on considering the imprecision of blind spots inherent in the overlapping of shots during the acquisition of photographs to be used as raw materials for the work of

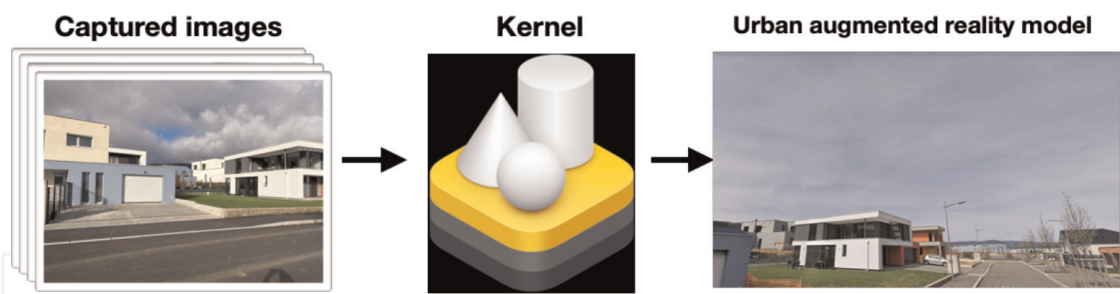


**Figure 6.**  
*Experimental UAR model for 3D spatial analysis.*

implementing augmented reality scenes. In addition, it provides a flexible architecture that fosters the development augmented reality applications about research in theoretical and quantitative geography like UAR.

4.2 Datasets and input quality analytics

The quality of data (accuracy, precision, and resolution) taken by sensors as smartphones is determined by many factors related to both the capture technique and the physical environment. Ideal physical conditions should favor diffused and homogeneous lighting and all protruding urban objects should have enough space around them. In addition, when taking photos, special attention should be paid to the following object/environment characteristics: sufficient texture detail and minimal reflective surfaces.

To select from the entire set of photographic data, the images meeting these criteria as well as those set out in **Table 1**, a valuation of the threshold values (high, and low) based on a fuzzy set as shown in **Figure 7**.

To ensure the quality of the input data, the input image quality sorting process consisted of sifting through the 1028 raw images captured for the entire study area. Indeed, the 800 photos organized in 799 pairs to constitute the input database are the result of the application of this cleaning process. Also, although variations in the quality of photogrammetric data are attributable to factors beyond the control of the operator, several steps can be taken to increase the likelihood that the data collected will achieve the desired quality. The following three points of vigilance are in order: 1) Consider the expected data collection conditions (e.g., weather, lighting), the quality of the camera and the lens. 2) Using the target range and camera specifications, calculate the desired spacing between successive frames to ensure adequate overlap. The interval [0.7–0.9] is the optimum since the value of 0.7 already gives excellent results. 3) After data collection, review and remove any poor quality/blurry images by manual or automatic means.

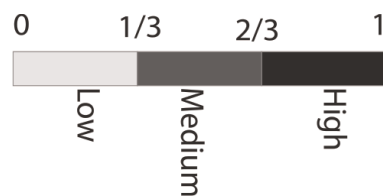


**Figure 7.**  
*Fuzzy set assigned to input image quality factor.*



### **4.3 Performance analytics and originality**

To evaluate and measure the performance of our FPAK approach associated with the ARKit rendering engine, the results obtained are compared with two other approaches [64, 87, 93, 95] on the same basis of the five constraints referenced in **Table 2**.

The first comparison model is the Deterministic Simulated Annealing (DSA) metaheuristics optimization algorithm. In Pajares and Cruz [95], this strategy for stereovision matching was exploited with satisfactory results. It is a comprehensive approach belonging to the category of methods that incorporate explicit smoothing assumptions and determine all disparities simultaneously by applying a energy minimization process. The limits of this approach are felt when the input database exceeds 82 pairs of stereo images and whose convergence is only reached after 30 iterations [87].

The second comparison model is based on the so-called relaxation labeling approach (RELB). This is a technique proposed by Rosenfeld et al. [98] to account for uncertainty in sensory data interpretation systems and to find the best matches. It uses contextual information as an aid to the classification of a set of interrelated objects by allowing interactions between possible classifications of related objects. In the stereovision paradigm, the problem is to assign unique labels (or matches) to a set of features in an image from a given list of possible matches.

The objective is to assign to each feature (edge segment) a value corresponding to the disparity in a way consistent with certain predefined constraints according to probabilities assigned to the five constraints in the studies [64, 93]. Here, the maximum number of input image pairs is increased to 90 for convergence from the 35th iteration. The results of performance comparison are synthesized in **Table 4**.

Although pioneering works [64, 87, 93, 95] have paved the way for the fuzzy modeling of the constraints inherent in image matching in stereovision applications, the originality of our work is assessed at three distinct levels. First, our method fits perfectly with a professional rendering engine such as ARKit. Second, the five constraints are modeled as concepts within the framework of FCMs. And third, the calculations did not require additional models as in the case of the DSA or RELB based approach. In doing so, the entire modeling chain constituted a fuzzy inference system.

## **5. Conclusion and future directions**

Computer-vision-based API (Application Programming Interface) such as ARKit enable landscape and urban physical feature capture on mobile devices like iPhone with a physically based rendering. They open new possibilities for applications, such as Virtual Geographic Environment (VGE) modeling for 3D spatial analysis. In this chapter, we explored one process of capturing urban built environment into an Urban Augmented Reality Model (UARM) and urban layouts according to the well-established soft computing framework Fuzzy Cognitive Map (FCM). It's a novel application of FCM which let us verify the performance and the robustness of our approach as compared to other existing methods.

Moreover, visualization of the urban development plan using UAR model gives one of the best augmented spatial models for urban planning simulation and 3D spatial analysis. In fact, the paradigm of augmented reality simplifies the process of project

Algorithm	Stereovision matching constraints for UAR modeling						
	Epipolar	Similarity	Smoothness	Ordering	Uniqueness	Maxi pairs of stereo images	Iterations need for Convergence
FPAK	Mapped as coefficients aggregated in the causal weight between concepts	Simple difference vector	Mapped as coefficients aggregated in the causal weight between concepts	Mapped as coefficients aggregated in the causal weight between concepts	Applied by selecting the highest causal concept values	799+	20
DSA	Mapped as an energy minimized by Simulated Annealing	Support Vector Machines	Mapped as an energy minimized by Simulated Annealing	Mapped as an energy minimized by Simulated Annealing	Applied by selecting the highest state value	82	30
RELB	Mapped under the overlapping concept	Bayes probability density estimation	Probabilistic relaxation	Probabilistic relaxation	Applied by selecting the highest probabilities	90	35

**Table 4.**  
*Synoptic performance comparison of FPAK with DSA and RELB.*

planning, measurement computations, design updates, collection of on-site architecture environment, safety training, etc.

Although UAR model uses multiple tools, it is the best visual aid to get walkthroughs for analyzing the virtual urban development plans. There are specific issues like high computational complexities, networking requirements and storage complexities to be considered. However, in practice, the limitations regarding technical issues can be overcome (to possible extents) as a scope for future research. The proposed method can further enhance the level of understanding of urban built environment by incorporating cloud computing services. We could realize uploading as well as synchronization of information contained in connected devices which feed smart cities.

Thus, the Architecture, Engineering, Construction, and Facility Management (AEC/FM) designs and construction site 3D visuals can be accessible, examinable, and modifiable from any location, irrespective of the location.

Users from different locations can collaborate with each other by accessing these cloud UARM services. The incorporation of cloud UARM for BIM's (Building Information Modeling) 3D visualization of construction layouts does elicit further investigation.

The performance assessment is still in progress. So, for detecting a possible bias of over- and underestimation of the five concepts of image matching due to ARKit, we are investigating two metrics: Mean Absolute Error (MAE) and the non-parametric Spearman's Rank Correlation Coefficient (SRCC).


## Author details

Igor Agbossou

Laboratoire ThéMA UMR 6049, Institut Universitaire de Technologie Nord  
Franche-Comté, Université de Franche-Comté, Belfort, France

\*Address all correspondence to: [igor.agbossou@univ-fcomte.fr](mailto:igor.agbossou@univ-fcomte.fr)

## IntechOpen

© 2023 The Author(s). Licensee IntechOpen. This chapter is distributed under the terms of the Creative Commons Attribution License (<http://creativecommons.org/licenses/by/3.0>), which permits unrestricted use, distribution, and reproduction in any medium, provided the original work is properly cited. 

## References

- [1] Batty M. *Cities and Complexity*. Cambridge: MIT Press; 2005
- [2] Batty M, Torrens P. Modelling and prediction in a complex world. *Futures*. 2005;**37**:745-766
- [3] Benenson I, Torrens P. *Geosimulation: Automata-Based Modelling of Urban Phenomena*. Chichester: Wiley; 2002
- [4] Berrou JL, Beecham J, Quaglia P, Kagarlis MA, Gerodimos A. Calibration and validation of the legion simulation model using empirical data. In: Aldau WN, Gattermann P, Knoflacher H, Schreckenber M, editors. *Pedestrian and Evacuation Dynamics*. New York: Springer Verlag; 2007. pp. 155-166
- [5] Portugali J. *Self-Organization and the City*. New York: Springer-Verlag; 2000
- [6] Ioannides YM, Zabel JE. Interactions, neighborhood selection and housing demand. *Journal of Urban Economics*. 2008;**63**:229-252
- [7] Couclelis H. The certainty of uncertainty: GIS and the limits of geographic knowledge. *Transactions in GIS*. 2003;**7**:165-175
- [8] Biswajeet P, editor. *Spatial Modeling and Assessment of Urban Form Analysis of Urban Growth: From Sprawl to Compact Using Geospatial Data*. Switzerland: Springer; 2017. p. 331. DOI: 10.1007/978-3-319-54217-1
- [9] Dicken P, Lloyd PE. *Location in Space: Theoretical Perspectives in Economic Geography*. New York: Harper and Row; 1990
- [10] Goodchild M. GIScience ten years after ground truth. *Transactions in GIS*. 2006;**10**:687-692
- [11] Longley PA, Goodchild MF, Maguire DJ, Rhind DW. *Geographic Information Systems and Science*. 2nd ed. Wiley and Sons: Chichester; 2005
- [12] Longley PA, Singleton AD. Social deprivation and digital exclusion in England. In: *CASA Working Paper*, 145. London: UCL Centre for Applied Spatial Analysis; 2008
- [13] Morrissey K, Clarke G, Hynes S, O'Donoghue C. Accessibility modelling. In: Bavaud F, Mager C, editors. *Handbook of Theoretical and Quantitative Geography*, FGSE, Lausanne, Switzerland: University of Lausanne; 2009. p. 457
- [14] Pumain D, Sanders L, Saint-Julien T. *Villes et auto-organisation*. Paris: Economica; 1989
- [15] Anders K-H. Level of detail generation of 3D building groups by aggregation and Typification. *International Cartographic Conference*. Vol. 2. 2005. Available from: <https://cite.seerx.ist.psu.edu/document?repid=rep1&type=pdf&doi=1f8df00d63c3008b90c68f32cdf498765c9d776d>
- [16] Batty M. *Visually-Driven Urban Simulations: Exploring Fast and Slow Changes in Residential London*, CASA, Working Papers Series. Vol. 164. London: UCL; 2011
- [17] Bazzanella L, Caneparo L, Corsico F, Roccasalva G, editors. *Future Cities and Regions. Simulation, Scenario and Visioning, Governance and Scales*. New York, Heidelberg: Springer; 2011
- [18] Bittner T, Donnelly M, Winter S. Ontology and semantic interoperability. In: Prosperi D, Zlatanova S, editors.



Large-Scale 3D Data Integration: Challenges and Opportunities. Boca Raton, FL: CRC Press; 2005

[19] Bucher B, Falquet G, Clementini E, Sester M. Towards a typology of spatial relations and properties for urban applications. Usage, Usability, and Utility of 3D City Models. 2012. p. 11. DOI: 10.1051/3u3d/201202010

[20] Gallagher J, Gill LW, McNabola A. Numerical modelling of the passive control of air pollution in asymmetrical urban street canyons using refined mesh discretization schemes. Building and Environment. 2012;56:232-240

[21] Raufirad V, Heidari Q, Ghorbani J. Comparing socioeconomic vulnerability index and land cover indices: Application of fuzzy TOPSIS model and geographic information system. Ecological Informatics. 2022;72:101917. DOI: 10.1016/j.ecoinf.2022.101917

[22] Agbossou I. Fuzzy cognitive maps-based modeling of residential mobility dynamics: GeoComputation approach. Plurimondi. 2017;17:169-190

[23] Agbossou I, Provitolo D, Frankhauser P. Expérimentation par voie informatique de la mobilité résidentielle, XVème Journées de Rochebrune. In: Rencontres interdisciplinaires sur les systèmes complexes naturels et artificiels. Rochebrune, Megève, France. CD Rom; 2008. pp. 1-13

[24] Agbossou I. Cerner le contexte spatial par les voisinages dans les modèles cellulaires en géographie. In: Rencontres interdisciplinaires sur le contexte dans les systèmes complexes naturels et artificiels, Jan 2010. Megève, France; 2010

[25] Marsala C, Bouchon-Meunier B. Entropies et ensembles flous

intuitionnistes. In: LFA 2019 - Rencontres francophones sur la Logique Floue et ses Applications. Alès, France: Cépaduès; 2019. pp. 143-148

[26] Coletti G, Bouchon-Meunier B. Fuzzy Similarity Measures and Measurement Theory. In: IEEE International Conference on Fuzzy Systems 2019 (FUZZ-IEEE 2019). New Orleans, United States: IEEE; 2019

[27] Abbasi F, Allahviranloo T, Abbasbandy S. A new attitude coupled with fuzzy thinking to fuzzy rings and fields. Journal of Intelligent & Fuzzy Systems. 2015;29:851-861

[28] Abbasi F, Abbasbandy S, Nieto JJ. A new and efficient method for elementary fuzzy arithmetic operations on pseudo-geometric fuzzy numbers. Journal of Fuzzy, Set Valued Analysis. 2016;2: 156-173

[29] Allahviranloo T, Mikaeilvand N. Non zero solutions of the fully fuzzy linear systems. Journal of Computational and Applied Mathematics. 2011;10(2): 271-282

[30] Jetter AJ, Kok K. Fuzzy Cognitive Maps for futures studies. A methodological assessment of concepts and methods, Futures. 2014;61:45-57, DOI: 10.1016/j.futures.2014.05.002.

[31] Liu ZQ, Satur R. Contextual fuzzy cognitive map for decision support in geographic information systems. IEEE Transactions on Fuzzy Systems. 1999;7(5):495-507

[32] Kosko B. Fuzzy Cognitive Maps. International Journal of Man-Machine Studies. 1986;24:65-75

[33] Kosko B. Neural Networks and Fuzzy Systems: A Dynamical Systems

Approach to Machine Intelligence. NJ: Prentice Hall; 1992

[34] Xirogiannis G, Stefanou J, Glykas M. A fuzzy cognitive map approach to support urban design. *Expert Systems with Applications*. 2004;**26**(2):257-268. DOI: 10.1016/S0957-4174(03)00140-4

[35] Unity Real-Time Development Platform. 3D, 2D VR & AR Engine. Available from: <https://unity.com/> [Accessed: November 19, 2021]

[36] blender.org—  
 Homeoftheblenderproject—  
 Freeandopen3Dcreationsoftware,  
 Available from: <https://www.blender.org/> [Accessed: September 12, 2021]

[37] Verma JK et al. *Advances in Augmented Reality and Virtual Reality, Studies in Computational Intelligence*. Springer; 2022. DOI: 10.1007/978-981-16-7220-0\_2

[38] Karthikeyan OVGSK, Padmanaban S, editors. *Smart Buildings Digitalization. Case Studies on Data Centers and Automation*. Abingdon, Oxon, OX14 4RN: CRC Press; 2022. p. 314. DOI: 10.1201/9781003240853

[39] Verma JK, Paul S, editors. *Advances in Augmented Reality and Virtual Reality*. Singapore: Springer; 2022. p. 312. DOI: 10.1007/978-981-16-7220-0

[40] Quan L. *Image-Based Modeling*. London: Springer; 2010. DOI: 10.1007/978-14419-6679-7

[41] Kuldip A, Dibyendu G. Nature inspired prototype Design of Collision Avoidance Aircraft System and Design of a pair of wing flaps in Autodesk Maya software. *Procedia Computer Science*. 2016;**89**:684-689. DOI: 10.1016/j.procs.2016.06.036

[42] Naiman JP. AstroBlend: An astrophysical visualization package for blender. *Astronomy and Computing*. 2016;**15**:50-60. DOI: 10.1016/j.ascom.2016.02.002

[43] Pelayo P et al. CubeSat landing simulations on small bodies using blender. *Advances in Space Research*. Volume 70, Issue 3 Elsevier, 2022. DOI: 10.1016/j.asr.2022.07.044

[44] Lars K, Leif K. Interactive modeling by procedural high-level primitives. *Computers & Graphics*. 2012;**36**(5):376-386. DOI: 10.1016/j.cag.2012.03.028

[45] Johannes E et al. Procedural modeling of architecture with round geometry. *Computers & Graphics*. 2017;**64**:14-25. DOI: 10.1016/j.cag.2017.01.004

[46] Andrew RW et al. Volumetric procedural models for shape representation. *Graphics and Visual Computing*. 2021;**4**:200018. DOI: 10.1016/j.gvc.2021.200018

[47] Gustavo A et al. Procedural modeling applied to the 3D city model of bogota: A case study. *Virtual Reality & Intelligent Hardware*. 2021;**3**(5):423-433. DOI: 10.1016/j.vrih.2021.06.002

[48] Mudit G et al. O-2 | development of a 3D modeling tool for procedural planning of ductal stenting. *Journal of the Society for Cardiovascular Angiography & Interventions*. 2022;**1**(3):100052. DOI: 10.1016/j.jscai.2022.100052

[49] Biljecki F, Ledoux H, Stoter J. Generating 3D city models without elevation data. *Computers, Environment and Urban Systems*. 2017;**64**:1-18

[50] Peeters A, Etzion Y. Automated recognition of urban objects for

morphological urban analysis. Computers, Environment and Urban Systems. 2012;**36**(6):573-582

[51] Goetz M, Zipf A. OpenStreetMap in 3D – Detailed insights on the current situation in Germany. In: Proceedings of the AGILE'2012 Inter- National Conference on Geographic Information Science. Avignon: AGILE Digital Editions; 2012. pp. 288-292

[52] Kim T-H et al. Smart city and IoT. Future Generation Computer Systems. 2017;**76**:159-162. DOI: 10.1016/j.future.2017.03.034

[53] Yonghuai L et al., editors. 3D Imaging, Analysis and Applications. Second ed. Switzerland: Springer; 2022. DOI: 10.1007/978-3-030-44070-1

[54] Boonsuk W, Gilbert SB, Kelly JW. The impact of three interfaces for 360- degree video on spatial cognition. In: Conference on Human Factors in Computing Systems — Proceedings. New York, USA: ACM Press; 2012. pp. 2579-2588

[55] Puyun L et al. A linear pushbroom satellite image epipolar resampling method for digital surface model generation. ISPRS Journal of Photogrammetry and Remote Sensing. 2022;**190**:56-68. DOI: 10.1016/j.isprsjprs.2022.05.010

[56] Remya R, Nirmala M. A novel similarity metric for image filtering. Optik. 2022;**271**:169977. DOI: 10.1016/j.ijleo.2022.169977

[57] Tahereh B et al. Edge preserving range image smoothing using hybrid locally kernel-based weighted least square. Applied Soft Computing. 2022; **125**:109234. DOI: 10.1016/j.asoc.2022.109234

[58] Xiang W et al. A novel reversible image data hiding scheme based on pixel

value ordering and dynamic pixel block partition. Information Sciences. 2015;**310**: 16-35. DOI: 10.1016/j.ins.2015.03.022

[59] Owen Saxton W. The image and diffraction plane problem: uniqueness, Reprinted from Advances in Electronics and Electron Physics, Supplement 10, 1978. In: Hýtch M, Hawkes PW, editors. Advances in Imaging and Electron Physics. Vol. 214. London: Elsevier; 2020. pp. 87-104. DOI: 10.1016/bs.aiep.2020.04.004

[60] Deepak G, Aditya K, Ashish K, Oscar C, editors. Soft Computing for Data Analytics, Classification Model, and Control. Switzerland AG: Springer; 2022. p. 165. DOI: 10.1007/978-3-030-92026-5

[61] Dadios EP, editor. Fuzzy Logic – Algorithms, Techniques and Implementations. London, UK, London, UK: InTech; 2012

[62] Allahviranloo T, Perfilieva I, Abbasi F. A new attitude coupled with fuzzy thinking for solving fuzzy equations. Soft Computing. 2018;**22**(9):3077-3095

[63] Abbasi F, Allahviranloo T. Computational procedure for solving fuzzy equations. Soft Computing. 2021; **25**:1-15. DOI:10.1007/s00500-020-05330-8

[64] Pajares G, de la Cruz JM. Fuzzy cognitive maps for stereovision matching. Pattern Recognition. 2006;**39** (11):2101-2114. DOI: 10.1016/j.patcog.2006.04.003

[65] Adeleke O, Jen T-C. A FCM-clustered neuro-fuzzy model for estimating the methane fraction of biogas in an industrial-scale bio-digester. Energy Reports. 2022;**8**(Supplement 15): 576-584. DOI: 10.1016/j.egy.2022.10.265



- [66] Hosseinpour M, Ghaemi S, Khanmohammadi S, Daneshvar S. A hybrid high-order type-2 FCM improved random forest classification method for breast cancer risk assessment. *Applied Mathematics and Computation*. 2022; **424**:127038. DOI: 10.1016/j.amc.2022.127038
- [67] Senthilkumar N et al. Minimally parametrized segmentation framework with dual metaheuristic optimisation algorithms and FCM for detection of anomalies in MR brain images. *Biomedical Signal Processing and Control*. 2022;**78**:103866. DOI: 10.1016/j.bspc.2022.103866
- [68] Kosko B. Hidden patterns in combined and adaptive knowledge networks. *International Journal of Approximate Reasoning*. 1988;**2**:377-393
- [69] Kosko B. Adaptive inference in fuzzy knowledge networks. In: Dubois D, Prade H, Yager RR, editors. *Readings in fuzzy sets for intelligent systems*. San Mateo: Morgan Kaufman; 1993
- [70] Eden C, Ackermann F, Brown I, Eden C, Ackermann F. *Making Strategy: The Journey of Strategic Management*. London: SAGE; 2006
- [71] Eden C, Ackermann F, Cropper S. The analysis of cause maps. *Journal of Management Studies*. 2007;**29**:309-324
- [72] Axelrod R. *Structure of Decision: The Cognitive Maps of Political Elites*. Princeton, NJ: Princeton University Press; 1976
- [73] Kowalski RM, Leary MR. *The Social Psychology of Emotional and Behavioral Problems: Interfaces of Social and Clinical Psychology*. États-Unis, American Psychological Association; 1999
- [74] Papageorgiou E, Stylios CD, Groumpos PP. Active Hebbian learning algorithm to train fuzzy cognitive maps. *International Journal of Approximate Reasoning*. 2004;**37**(3):219-249
- [75] Papageorgiou E, Stylios CD, Groumpos PP. Fuzzy cognitive map learning based on nonlinear Hebbian Rule. In: Gedeon TD, Fung LCC, editors. *AI 2003: Advances in Artificial Intelligence*. AI 2003. Lecture Notes in Computer Science. Vol. 2903. Berlin, Heidelberg: Springer; 2003. DOI: 10.1007/978-3-540-24581-0\_22
- [76] Wang Y, Liqiang Z, Takis Mathiopoulos P, Deng H. A gestalt rules and graph-cut-based simplification framework for urban building models. *International Journal of Applied Earth Observation and Geoinformation*. 2015; **35**(Part B):247-258. DOI: 10.1016/j.jag.2014.09.012
- [77] Fang Y, Zhang X, Yuan F, Imamoglu N, Liu H. Video saliency detection by gestalt theory. *Pattern Recognition*. 2019;**96**:106987. DOI: 10.1016/j.patcog.2019.106987
- [78] Xue T, Owens A, Scharstein D, Goesele M, Szeliski R. Multi-frame stereo matching with edges, planes, and superpixels. *Image and Vision Computing*. 2019;**91**:103771. DOI: 10.1016/j.imavis.2019.05.006
- [79] Szeliski R. *Computer Vision: Algorithms and Applications*, Texts in Computer Science. London: Springer; 2011. DOI: 10.1007/978-1-84882-935-0
- [80] Lopes A, Souza R, Pedrini H. A survey on RGB-D datasets. *Computer Vision and Image Understanding*. 2022; **222**:103489. DOI: 10.1016/j.cviu.2022.103489
- [81] Scharstein D, Briggs AJ. Real-time recognition of self-similar landmarks. *Image and Vision Computing*. 2001;**19**



(11):763-772. DOI: 10.1016/S0262-8856(00)00105-0

[82] Cherdo L. The 8 Best 3D Scanning Apps for Smartphones and iPads in 2019. 2019. Available from: <https://www.aniwaa.com/buyers-guide/3d-scanners/best-3d-scanning-apps-smartphones/> [Accessed: May 12, 2022]

[83] Wang D. The time dimension for scene analysis. *IEEE Transactions on Neural Networks*. 2005;**16**(6):1401-1426

[84] Li Z, Yan H, Ai T, Chen J. Automated building generalization based on urban morphology and gestalt theory. *International Journal of Geographical Information Science*. 2004;**18**(5):513-534. DOI: 10.1080/13658810410001702021

[85] Reimer LM, Weigel S, Ehrenstorfer F, Adikari M, Birkle W, Jonas S. Mobile motion tracking for disease prevention and rehabilitation using apple ARKit. In: Hayn D, Schreier G, Baumgartner M, editors. *Studies in Health Technology and Informatics*. Amsterdam, The Netherlands: IOS Press; 2021. DOI: 10.3233/SHTI210092

[86] Zhou X, Leonardos S, Hu X, Daniilidis K. 3D shape estimation from 2D landmarks: A convex relaxation approach. In: *Proceedings of the 2015 IEEE Conference on Computer Vision and Pattern Recognition (CVPR)*, Boston, MA, USA, 7–15 June 2015. Boston, MA, USA: IEEE; 2015. pp. 4447-4455. DOI: 10.1109/CVPR.2015.7299074

[87] Javier Herrera P, Pajares G, Guijarro M, Ruz JJ, de la Cruz JM. Combining support vector machines and simulated annealing for stereovision matching with fisheye lenses in forest environments. *Expert Systems with Applications*. 2011;**38**(7):8622-8631. DOI: 10.1016/j.eswa.2011.01.066

[88] Liu Y, Wang W, Xintao X, Guo X, Gong G, Huaxiang L. Lightweight real-time stereo matching algorithm for AI chips. *Computer Communications*. 2022;**199**:210-217. DOI: 10.1016/j.comcom.2022.06.018

[89] Yuan W, Meng C, Tong X, Li Z. Efficient local stereo matching algorithm based on fast gradient domain guided image filtering. *Signal Processing: Image Communication*. 2021;**95**:116280. DOI: 10.1016/j.image.2021.116280

[90] Wilm J, Aanæs H, Larsen R, Paulsen RR. *Real Time Structured Light and Applications*. Kgs. Lyngby: Technical University of Denmark (DTU), 2016 (DTU Compute PHD-2015; No. 400);

[91] Scharstein D, Szeliski R. A taxonomy and evaluation of dense two-frame stereo correspondence algorithms. *International Journal of Computer Vision*. 2002;**47**(1):7-42

[92] Hirschmuller H, Scharstein D. Evaluation of stereo matching costs on images with radiometric differences. *IEEE Transactions on Pattern Analysis and Machine Intelligence*. 2008;**31**(9): 1582-1599

[93] Pajares G, de la Cruz JM, López-Orozco JA. Relaxation labeling in stereo image matching. *Pattern Recognition*. 2000;**33**(1):53-68. DOI: 10.1016/S0031-3203(99)00036-9

[94] Ma X-L, Yuan R-Y, Zhang L-B, He M-Y, Zhang H-L, Xing Y, et al. Augmented reality autostereoscopic 3D display based on sparse reflection array. *Optics Communications*. 2022;**510**: 127913. DOI: 10.1016/j.optcom.2022.127913

[95] Pajares G, de la Cruz JM. On combining support vector machines and simulated annealing in stereovision

matching. IEEE Transactions on Systems, Man, and Cybernetics. Part B, Cybernetics. 2004;**34**(4):1646-1657.  
DOI: 10.1109/tsmcb.2004.827391

[96] Dive into the world of augmented reality [Internet]. 2022. Available from: <https://developer.apple.com/augmented-reality> [Accessed: October 14, 2021]

[97] RealityKit. Simulate and render 3D content for use in your augmented reality apps [Internet]. 2022. Available from <https://developer.apple.com/documentation/realitykit> [Accessed: October 15, 2021]

[98] Rosenfeld A, Hummel RA, Zucker SW. Scene labeling by relaxation operations. In: IEEE Transactions on Systems, Man, and Cybernetics. Vol. SMC-6. June 1976. no. 6. pp. 420-433, DOI: 10.1109/TSMC.1976.4309519